On the Role of Methyl Torsional Modes in the Intersystem Crossing Dynamics of Isolated Molecules†

Leonardo Alvarez-Valtierra, Xue-Qing Tan, and David W. Pratt*

Department of Chemistry, University of Pittsburgh, Pittsburgh, Pennsylvania 15260

Received: August 15, 2007; In Final Form: September 15, 2007

Rotationally resolved fluorescence excitation spectra of the 0_0^0 bands of the $S_1 \leftarrow S_0$ electronic transitions of 2- and 5-methylpyrimidine (2MP and 5MP, respectively) have been observed and assigned. Both spectra were found to contain two sets of rotational lines, one associated with the $\sigma = 0$ torsional level and the other associated with the $\sigma = \pm 1$ torsional level of the attached methyl group. Analyses of their structure using the appropriate torsion−rotation Hamiltonian yields the methyl group torsional barriers of $V_6'' = 1.56$ and $V_6' = 8.28$ cm^{-1} in 2MP and $V_6'' = 4.11$ and $V_6' = 58.88$ cm^{-1} in 5MP. Many of the lines in both spectra are fragmented by couplings with lower lying triplet states. Analyses of some of these perturbations yield approximate values of the intersystem crossing matrix elements, from which it is concluded that the $\sigma = \pm 1$ torsional levels of the S_1 state are significantly more strongly coupled to the T_1 state than the $\sigma = 0$ torsional levels.

1. Introduction

Reported here are studies at high resolution of the $S_1 \leftarrow S_0$ fluorescence excitation spectra of 2-methylpyrimidine (2MP) and 5-methylpyrimidine (5MP) as isolated species in the collision-free environment of a molecular beam. Pyrimidine itself lies close to the small molecule limit in the language of radiationless transitions. It exhibits a zero-pressure fluorescence quantum yield of ∼0.3 and a fluorescence decay that exhibits quantum beats, owing to spin−orbit coupling with a lower triplet state.[1] Hence, we reasoned that attachment of a single methyl group to pyrimidine might influence this process, by providing a low frequency torsional coordinate along which state densities and/or coupling matrix elements might be enhanced. If this proves to be true, then 2MP and 5MP might be transformed into intermediate-case molecules with a significantly lower quantum yield and biexponential decay behaviors and exhibit "intrinsically unassignable" high-resolution spectra.

A radiationless transition is a change in the electronic state of a molecule that occurs without the absorption or emission of radiation. In bound states, there are two processes of this type, internal conversion (IC) and intersystem crossing (ISC). There has been a tremendous amount of research directed toward the study of these phenomena in the past 50 years. (Early work in the field has been reviewed by Kommandeur et al.)[2] Radiationless transitions in a polyatomic molecule occur via the transfer of energy from one multidimensional potential energy surface to another and therefore are related to all types of chemical transformations. Intramolecular vibrational relaxation (IVR) is a related process that occurs on a single surface, which results in an apparent energy flow from one mode into another.[3]

IVR, IC, and ISC are usually described by two sets of zero-order levels, a bright state $|s\rangle$ that carries the oscillator strength and a bath of nearly isoenergetic dark states $\{|k\rangle\}$ to which the bright state is coupled; see Figure 1. The decay behavior of the prepared state depends upon the energy level density ρ_k, the decay widths, γ_k and the $|s\rangle$ - $\{|k\rangle\}$ couplings v_{sk}. The important parameters characterizing the different molecular limits are $x_k = \rho_k\gamma_k$ and $v_{sk}^2\rho_k^2$. If $x_k \ll 1$, the average level spacing ϵ_k is large compared with the radiative decay width γ_k. If there are no (or only a few) couplings between the two manifolds, then the initial state decays exponentially (sometimes showing quantum beats) with a rate that is equal to (or slightly less than) the radiative rate, and the emission quantum yield is high. This is the small molecule limit ($v_{sk}^2\rho_k^2 \ll 1$). If $x_k \gg 1$, the average level spacing is small; if, further, $((v_{sk}^2/\epsilon_k)) \gg \gamma_s$, then there are a large number of couplings between the two manifolds, and the oscillator strength is spread out over a large number of levels. If only a fraction of these are contained within the excitation bandwidth, then the initial state decays exponentially with a rate that is faster than the radiative rate, and the emission quantum yield is low. This is the large molecule or statistical limit.

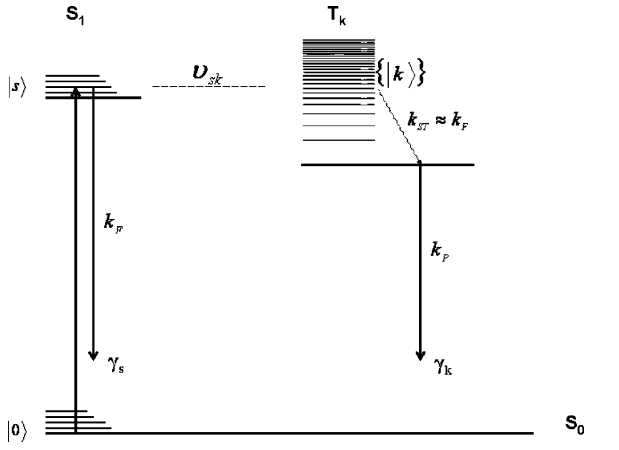

Figure 1. Radiationless transitions in a large molecule. $|s\rangle$ denotes the bright state that is optically prepared by excitation of the ground state $|0\rangle$, and coupled via matrix elements v_{sk} to a dense manifold of nearly isoenergetic dark states $\{|k\rangle\}$. In ISC, S_1 and T_k are zero-order singlet and triplet states, respectively.

† Part of the "Giacinto Scoles Festschrift".

* Corresponding author: pratt@pitt.edu.

10.1021/jp076568c CCC: $37.00
Published on Web 11/01/2007

As is often the case in science, valuable insight into the nature of dynamical processes is gained by studies of molecules that lie between the two limits, in the so-called "intermediate case". In such cases, radiationless transitions occur but are "reversible", and the decays are frequently non-exponential. A beautiful illustration of these effects can be found in the early work of Tramer and co-workers on pyrazine[4] and McDonald and co-workers on biacetyl.[5] ter Horst et al.[6] and Matsumoto et al.[7] showed that the decay behavior of pyrazine is strongly dependent on the rotational state and the presence of magnetic fields. However, probably the most dramatic demonstration of the existence of radiationless processes was provided by the direct detection of the fragmentation of a single zero-order bright state into two or more molecular eigenstates using high-resolution laser techniques; in benzene by Riedle et al.,[8] in pyrimidine by Konings et al.,[9] and in pyrazine by van der Meer et al.[10] The analogous observation of IVR-induced fragmentation of C−H stretching modes in several small organic molecules was observed by Perry and co-workers,[11] McIlroy and Nesbitt[12] and Lehmann and co-workers[13−14] at about the same time.

The increased level of detail provided by frequency-domain methods gives a more complete picture of energy redistribution processes. Much has been learned from studies of such spectra, including the measurements of relaxation rates and whether or not the process can be "manipulated" by excitation of certain modes, and not others. Scoles and his group have made notable contributions in this area, demonstrating in particular a "chromophore dependence of IVR" in several systems. Moore and co-workers[15] have reported similar studies of promoting modes in the photodissociation of D_2CO and related small molecules. But analogous studies of promoting modes in the corresponding electronic processes of IC and ISC are lacking in larger molecules. This is the purpose of the work described here.

2. Experimental Section

2MP (>99% pure) was obtained from Koei Chemical Company and 5MP (99% pure) was purchased from Sigma. Both chemicals were used without further purification. Dry argon and helium were used in all experiments as inert carrier gases.

In the vibrationally resolved experiments, samples were seeded into 40 psi of helium gas and expanded into a vacuum chamber (10^{-5} Torr) through a 1 mm diameter orifice pulsed valve (General Valve Series 9) operating at 10 Hz. Two centimeters downstream of the valve, the free jet was excited with the second harmonic of a Quanta Ray Nd^{3+}:YAG (model DCR-1A) pumped dye laser (model PDL-1). The dye (DCM) laser output was frequency doubled with an external potassium dihydrogen phosphate (KDP) crystal providing a spectral resolution of ~0.6 cm^{-1} in the ultraviolet (UV) region. From the point of intersection between the jet and the laser beam, the molecules were excited, and the fluorescence was collected with a photomultiplier tube (PMT). Finally, the collected data were processed by a boxcar integrator (Stanford Research Systems) and recorded with Quick Data Acquisition software (Version 1.0.5).

Rotationally resolved electronic experiments were performed using a molecular beam laser spectrometer, described in detail elsewhere.[16] Briefly, the molecular beam was formed by expansion of the vaporized sample (either 2MP or 5MP) seeded in argon carrier gas (−17 psi) through a heated (~330 K) 200 μm quartz nozzle into a differentially pumped vacuum system. The expansion was skimmed 2 cm downstream with a 1 mm diameter skimmer and crossed 13 cm further downstream by a continuous wave (CW) Ar^+ pumped ring dye laser. The CW laser was operated with DCM dye, and intracavity frequency doubled in a $LiIO_3$ crystal, yielding ~300 μW of UV radiation with a spectral resolution of about 1 MHz.

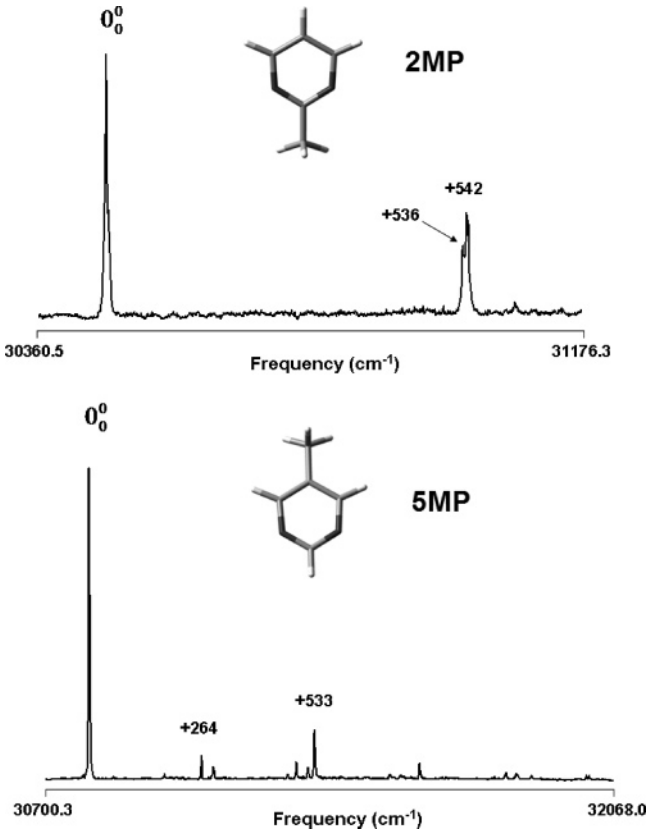

Figure 2. Vibrationally resolved fluorescence excitation spectra of 2MP and 5MP in the gas phase.

The fluorescence excitation spectrum was detected using spatially selective optics by a PMT and photon counting system. The PMT signal together with the iodine absorption spectrum and the relative frequency markers were simultaneously collected and processed by the JBA95 data acquisition system.[16] Absolute frequency calibration of the spectra was performed by comparison with the I_2 absorption spectrum. The relative frequency markers were obtained from a stabilized etalon with a free spectral range of 299.7520 ± 0.0005 MHz.

3. Results

Figure 2 shows the vibrationally resolved fluorescence excitation spectra of 2MP and 5MP in the gas phase. Like Zwier and co-workers,[17,18] we observe strong 0_0^0 transitions and no torsional bands near the electronic origins of either molecule. The origin (0_0^0) band in 2MP is at 30459.1 cm^{-1} (~328.3 nm), red-shifted from that of pyrimidine[7] by 614 cm^{-1}; whereas the 0_0^0 band in 5MP is at 30799.9 cm^{-1} (~324.7 nm), only 273 cm^{-1} red-shifted from the origin band of pyrimidine. The absence of Franck−Condon progressions along the low-frequency methyl torsional coordinate indicates that the preferred methyl group orientation is the same in both electronic states. The vibronic bands observed at about 535 cm^{-1} mainly correspond to the $6a_0^1$ mode combined with torsional levels to give rise to the splitting observed in the 2MP spectrum.[18]

We have performed extensive studies of these spectra at high resolution, to examine the dynamic properties of their electronically excited states. Figure 3 shows the rotationally resolved $S_1 \leftarrow S_0$ fluorescence excitation spectrum of the origin band of

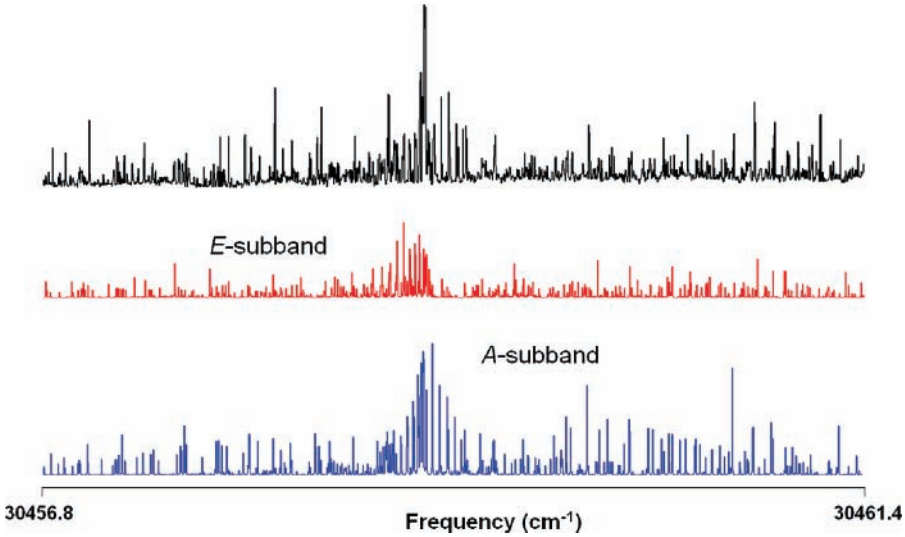

Figure 3. Rotationally resolved fluorescence excitation spectrum of 2MP in the gas phase. Two simulated spectra (*A* and *E* sub-bands), due to the methyl group internal rotation, are required to fit the experimental trace. The splitting of the two sub-bands is about 157 MHz.

2MP in the gas phase. The entire spectrum contains about 3000 rovibronic lines and spans approximately 4.5 cm^{-1} at a rotational temperature of about 5 K. Under the expansion conditions used in our experiments, only the lowest torsional levels ($\sigma = 0, \pm 1$) of 2MP are populated. Therefore, the transitions observed in the spectrum of Figure 3 are composed of two sub-bands, one associated with the $\sigma = 0$ (the *A* sub-band) and another with the $\sigma = \pm 1$ torsional levels (the *E* sub-band). The *A* sub-band was identified and assigned first and fit using rigid asymmetric rotor Hamiltonians for both electronic states. The fitting procedure was carried using the program *lbrot*,[19] which utilizes low barrier Hamiltonians and the graphic interface of JB95 fitting program.[20] The spectrum was found to be a pure *c*-type spectrum; the electronic transition moment vector is perpendicular to the plane of the aromatic ring. The final fit for the *A* sub-band utilized 129 rovibronic transitions and resulted in a standard deviation of 8.7 MHz; however, by performing a combination differences fitting procedure the standard deviation of the fit was reduced to 4.3 MHz.

The *E* sub-band contains rovibronic transitions whose degeneracies are lifted by the torsion−rotation interaction. Therefore, it was fit using the low barrier torsion−rotation Hamiltonian for a G_{12} molecule,[21−23]

$$\hat{H} = \hat{H}_T + \hat{H}_R + \hat{H}_{TR} \quad (1)$$

with

$$\hat{H}_T = Fp^2 + (1/2)V_6(1 - \cos 6\alpha) \quad (2)$$

$$\hat{H}_R = AP_z^2 + BP_x^2 + CP_y^2 + FP^2 \quad (3)$$

and

$$\hat{H}_{TR} = -2FPp \quad (4)$$

Here, the torsional ($\hat{H}_T$) and the rotational ($\hat{H}_R$) Hamiltonians are treated separately, with the use of an extra term ($\hat{H}_{TR}$) that couples them. $A = \hbar^2/2I_z$, and so forth, are the rigid rotor rotational constants, $P = \sum_g \lambda_g (I_\alpha/I_g) P_g$ is the total angular momentum of the methyl rotor, and $\lambda_g (g = x,y,z)$ are the direction cosines of the symmetry axis of the methyl rotor with respect to the principal axes of inertia. α is the internal-rotation coordinate, p is the torsional angular momentum, F is the methyl group rotational constant, and V_6 is the sixfold potential barrier height hindering the torsional motion.[24] The reported microwave values for the S_0 rotational constants and the corresponding barrier heights were taken as initial estimates for the fit of the experimental trace.[25] The final fit utilized 84 lines and resulted in a standard deviation of 15.5 MHz. The *E* sub-band was found to be red-shifted from the *A* sub-band by ~157 MHz. A portion of the *Q* branch of this spectrum is shown in Figure 4, where the need for the two independent simulated spectra is clearly evident. Individual lines exhibit Voigt profiles, with 18 MHz Gaussian and 40 MHz Lorentzian contributions. The inertial parameters obtained from the fits are summarized in Table 1.

Also apparent in Figure 4 are significant differences between the experimental spectrum and the calculated one, highlighted by boxes. These differences include "missing" transitions that appear in the simulated spectrum (Figure 4b) and "extra" transitions that appear in the experimental spectrum (Figure 4a). These observations are a direct consequence of spin−orbit coupling to a lower triplet state.

Figure 5 shows the rotationally resolved fluorescence excitation spectrum of the 0_0^0 band of 5MP in the gas phase. The spectrum spans about 4 cm^{-1} and contains more than 2000 rovibronic lines. Upon a similar analysis, two sub-torsional bands were also found in the spectrum of 5MP; the *A* sub-band was fit using rigid rotor Hamiltonians in both electronic states, whereas the *E* sub-band required the first-order torsion−rotation coupling terms described above. For this molecule, the *E* sub-band was observed to be red-shifted but by a larger magnitude (~7800 MHz) than in 2MP, which signals a larger difference in the methyl torsional barriers upon electronic excitation. This confirms the earlier results of Bandy et al.[17] and Bitto and Gfeller.[26] Both sub-torsional bands in 5MP exhibit pure *c*-type rovibronic transitions. The final fit for the *A* sub-band utilized 116 transitions and yielded a standard deviation of 7.49 MHz, which was improved to 4.22 MHz after a combination difference analysis. On the other hand, the *E* sub-band utilized 80 transitions and resulted in a standard deviation of 9.86 MHz. Figure 6 shows a portion of the experimental spectrum in a section where the two spectra overlap, including the two simulated *A* and *E* sub-bands. Note that this spectrum also exhibits several singlet−triplet perturbations. The inertial parameters obtained from the fits of the spectra of 5MP are reported in Table 2.

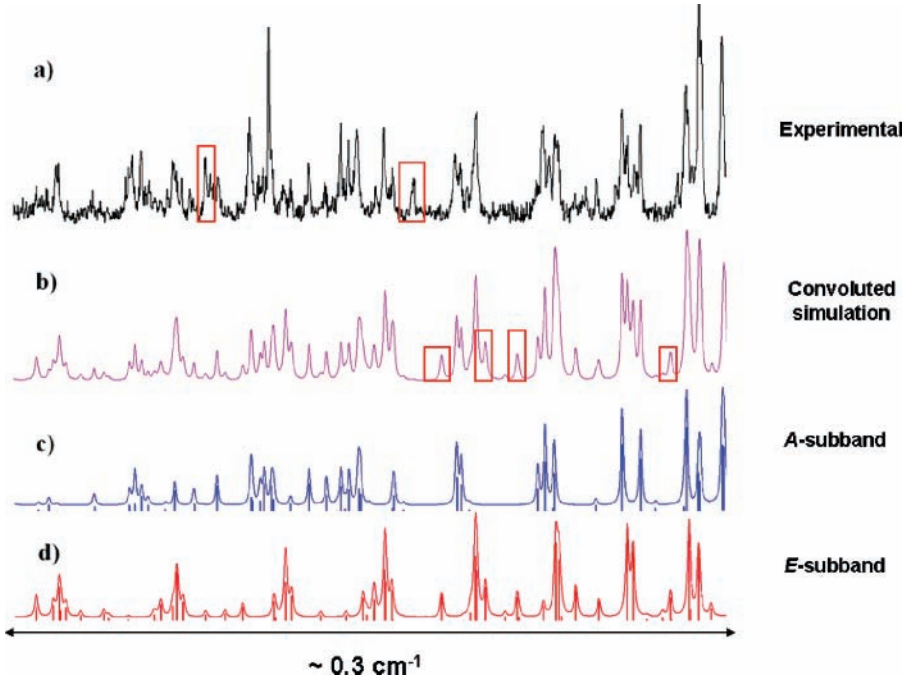

Figure 4. Portion of the *Q* branch in the origin band of the $S_1 \leftarrow S_0$ electronic spectrum of 2MP illustrating the quality of the fit. The experimental spectrum is shown in (a), the corresponding simulated spectrum is shown in (b), and the contributions of the two sub-bands are shown separately in (c) and (d). Boxes denote either "extra" transitions in (a) or "missing" transitions in (b).

TABLE 1: Inertial Parameters Derived from Fits of the High-Resolution Spectra of the *A* and *E* Subtorsional Bands of 2-Methylpyrimidine

parameter[a]	*E* sub-band	*A* sub-band	microwave[b]
S_0			
***A*″ MHz)**	6106.4 (1)	6095.6 (1)	6096.9 (1)
***B*″ (MHz)**	2770.3 (1)	2751.6 (1)	2751.7 (<1)
***C*″ (MHz)**	1867.7 (1)	1895.5 (1)	1895.6 (<1)
$\Delta I''$ (amu Å^2)	5.40 (5)	0.04 (5)	0.06
S_1			
***A*′ (MHz)**	6397.8 (1)	6373.4 (1)	
***B*′ (MHz)**	2600.1 (1)	2590.2 (1)	
***C*′ (MHz)**	1823.7 (1)	1842.0 (1)	
$\Delta I'$ (amu Å^2)	3.76 (5)	−1.04 (5)	
band origin (cm^{-1})	30459.06	30459.07	
OMC (MHz)	15.57	4.35	
temp (K)	4.5	4.5	

[a] Numbers in parentheses are the standard deviations of the last significant figure. [b] Values taken from ref 25.

TABLE 2: Inertial Parameters Derived from Fits of the High-Resolution Spectra of the *A* and *E* Subtorsional Bands of 5-Methylpyrimidine

parameter[a]	*E* sub-band	*A* sub-band	microwave[b]
S_0			
***A*″ MHz)**	6100.6 (1)	6108.3 (1)	6108.4 (1)
***B*″ (MHz)**	2640.5 (1)	2642.4 (1)	2642.2 (<1)
***C*″ (MHz)**	1847.6 (1)	1844.5 (1)	1844.2 (<1)
$\Delta I''$ (amu Å^2)	−0.69 (5)	0.00 (5)	0.03
S_1			
***A*′ (MHz)**	6357.8 (1)	6365.2 (1)	
***B*′ (MHz)**	2537.2 (1)	2538.9 (1)	
***C*′ (MHz)**	1818.9 (1)	1817.1 (1)	
$\Delta I'$ (amu Å^2)	−0.83 (5)	−0.32 (5)	
band origin (cm^{-1})	30799.63	30799.89	
OMC (MHz)	9.86	4.22	
temp (K)	5.0	5.0	

[a] Numbers in parentheses are the standard deviations of the last significant figure. [b] Values taken from ref 27.

Finally, we have been able to obtain both vibrationally and rotationally resolved electronic spectra of 4-methylpyrimidine (4MP), which are not reported here. The acquisition and analysis of this spectrum is in the process of being improved, since the fluorescence quantum yield in 4MP seems to be extremely small.

4. Discussion

4.1. Molecular Structures Upon Excitation. Tables 1 and 2 list the measured rotational constants of 2MP and 5MP in their ground and electronically excited states. The ground state values are in excellent agreement with the earlier microwave ones.[25,27] But the excited-state values are quite different, owing to light-induced changes in the molecular geometries of the two species. 2MP has ΔA ($A' - A''$), ΔB, and ΔC values of 277.8, −161.4, and −53.5 MHz, whereas 5MP has ΔA, ΔB, and ΔC values of 256.9, −103.4, and −27.4 MHz, respectively. (Both sets of values are from the *A* sub-band fits; the *E* sub-band values are slightly different owing to the second-order torsion−rotation contributions.) The results for both molecules provide evidence for significant contractions along directions perpendicular to *a*, and expansions along directions perpendicular to *b* and *c* when the photon is absorbed.

MP2 (second order Moller−Plesset) and CIS (configuration interaction-singles) ab initio calculations[28] were performed to determine the preferred orientation of the attached methyl group with respect to the plane of the ring in both electronic states. These calculations predict that the staggered orientation of the methyl (i.e., one of the C−H bonds is perpendicular to the plane of the ring) is preferred in both states, by a few wavenumbers of energy. A similar result has been obtained for toluene.[29]

Experimentally, the $S_1 \leftarrow S_0$ transition dipole moment vectors in both 2MP and 5MP were found to be oriented perpendicular to the plane of the aromatic ring (i.e., only pure *c*-type rovibronic transitions were observed). Figure 7 illustrates the results obtained from the CIS calculations. In agreement with our observations, the pictures of the MOs for both molecules signal an evident transition from an *n* orbital (no node in the plane of the ring and highly localized in the nitrogen atoms) to a π^* orbital (benzene-like LUMO).

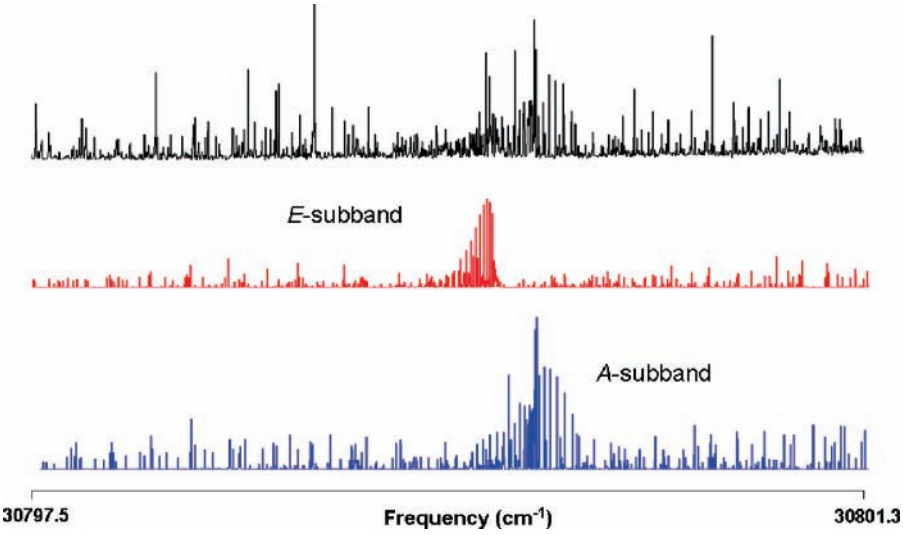

Figure 5. Rotationally resolved fluorescence excitation spectrum of 5MP in the gas phase. Two simulated spectra (*A* and *E* sub-bands), due to the methyl internal rotation, are required to fit the experimental trace. The splitting of the two sub-bands is about 7,800 MHz.

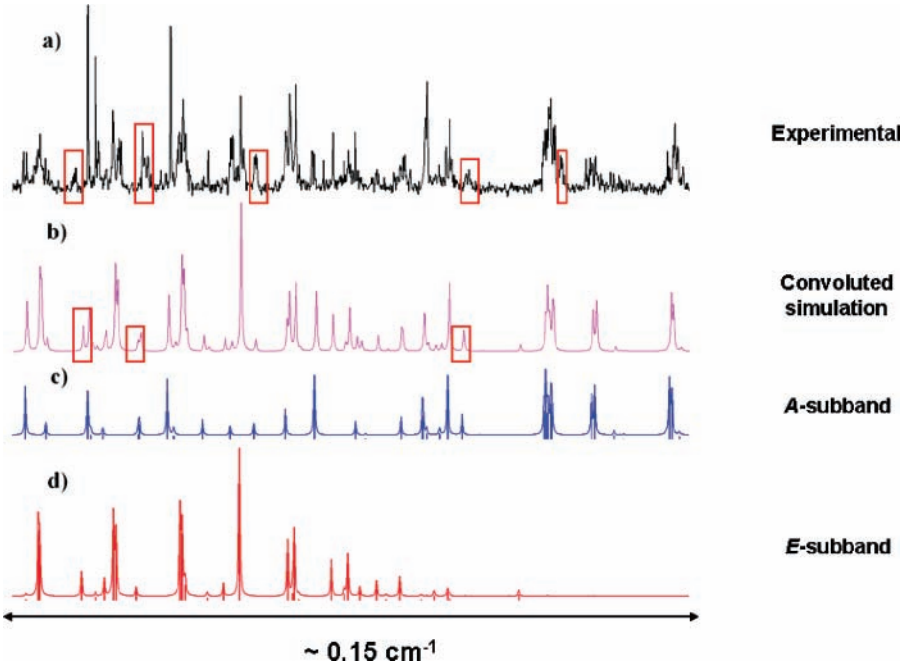

Figure 6. Portion of the *Q* branch in the origin band of the $S_1 \leftarrow S_0$ electronic spectrum of 5MP illustrating the quality of the fit. The experimental spectrum is shown in (a), the corresponding simulated spectrum is shown in (b), and the contributions of the two sub-bands are shown separately in (c) and (d). Boxes denote either "extra" transitions in (a) or "missing" transitions in (b).

Transfer of charge from the nitrogen lone pair(s) to the π^* orbital of the ring produces significant structural changes in the isolated molecules. For example, the calculations suggest that the N_1-C_2 and C_2-N_3 bonds shorten by ~0.04 Å (from 1.34 to 1.30 Å), the $N_1-C_2-N_3$ angle decreases by ~11° (from 126° to 115°) in both molecules, and the N_1-C_6 and N_3-C_4 bond lengths increase by ~0.02 Å. [Interestingly, in the methyl eclipsed configurations (geometry-optimized calculations performed by maintaining the methyl group torsional coordinate frozen), there is a remarkable difference in bond lengths of the N_1-C_2 and C_2-N_3 bonds in 2MP and C_5-C_6 and C_4-C_5 bonds in 5MP. Note that the only difference among these bonds is the relative orientation of the methyl group in the structures. Specifically, the C_5-C_6 bond is ~0.03 Å shorter than the C_4-C_5 bond in 5MP.] These structural changes are very different from those in the typical excitation of a $\pi\pi^*$ state in an aromatic molecule.[30]

4.2. Methyl Group Torsional Barriers. The torsional barriers hindering the rotation of the methyl group about either the C_2-C_{Methyl} bond in 2MP or the C_5-C_{Methyl} bond in 5MP were determined from the relative spacing in frequency of the *A* and *E* sub-torsional bands in the high-resolution spectra. The ground state torsional barriers, $V_6'' = 1.56$ for 2MP and $V_6'' = 4.11$ cm^{-1} for 5MP, were taken from more accurate microwave results.[25,27] Then, the excited-state torsional barriers, $V_6' = 8.28$ for 2MP and $V_6' = 58.88$ cm^{-1} for 5MP, were determined from the *A*−*E* splittings. The excited-state barrier in 5MP is significantly larger than that in 2MP. Plots of the one-dimensional torsional energy surfaces along the torsional coordinate for 2MP and 5MP in both electronic states are shown in Figure 8. Note, that the lower the torsional barrier heights, the closer the experimental inertial defects to zero (cf. Tables 1 and 2). A similar trend was observed in 2- and 3-methylanisole.[31]

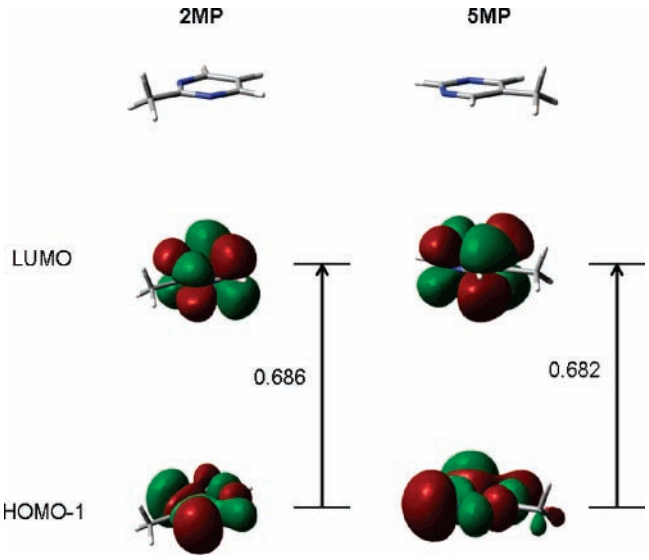

Figure 7. CIS/6-31G(d,p) frontier molecular orbitals with their corresponding transition probabilities in 2-methylpyrimidine (2MP) and 5-methylpyrimidine (5MP).

We believe that the observed methyl torsional barrier heights have their origin in π bond order differences of two neighboring ring covalent bonds in the eclipsed configuration of these molecules. To further investigate this phenomenon, the π covalent bond orders have been computed for both molecules in both staggered and eclipsed configurations in both electronic states.[32] When the methyl group is staggered in 2MP, the π bond orders of the N_1-C_2 and C_2-N_3 bonds are identical; $\rho_{12} = \rho_{23} = 0.458$ in S_0 and $\rho_{12} = \rho_{23} = 0.313$ in S_1. However, when the methyl group is eclipsed, the N_1-C_2 bond, the N_1-C_2 and C_2-N_3 covalent bond orders are no longer the same; $\rho_{12} = 0.510$ and $\rho_{23} = 0.409$ in the S_0 state, and $\rho_{12} = 0.367$ and $\rho_{23} = 0.259$ in the S_1 state. The difference in the two bond orders increases slightly from 0.101 in the S_0 state to 0.108 in the S_1 state, thereby explaining the small increase in V_6 in the electronically excited state. In contrast, the corresponding C_4-C_5 and C_5-C_6 covalent π bond order differences in 5MP are 0.180 and 0.438 for the S_0 and S_1 states, respectively, thereby accounting for the much larger increase in V_6 when 5MP absorbs light.

4.3. Intersystem Crossing Dynamics. The intersystem crossing dynamics in 2MP and 5MP are revealed in Figures 4 and 6. There, it was shown that the experimental spectra exhibit "extra" lines that do not appear in the simulations, which otherwise account for most of the observed intensity. At the same time, the simulations contain "missing" lines that that do not appear in the experimental spectra. Both of these observations can be explained by interactions between the zero-order singlet state and an otherwise dark manifold of triplet states, the "talisman" of ISC. A similar effect has been observed in pyrimidine.[9]

Though qualitatively similar, the high-resolution spectra of the two pyrimidine derivatives are quantitatively different from the spectra of the parent molecule. In pyrimidine itself, the number of extra lines is very small, typically 0−2 per zero-order state, and the fractional intensity that they exhibit is also very small, ∼0−5%.[9] 2MP and 5MP exhibit, in contrast, many more extra lines with significantly higher intensity, betraying the existence of a larger number of perturbations between the zero-order states. The spectra of 2MP and 5MP are still quite far from the statistical limit, as individual transitions can still

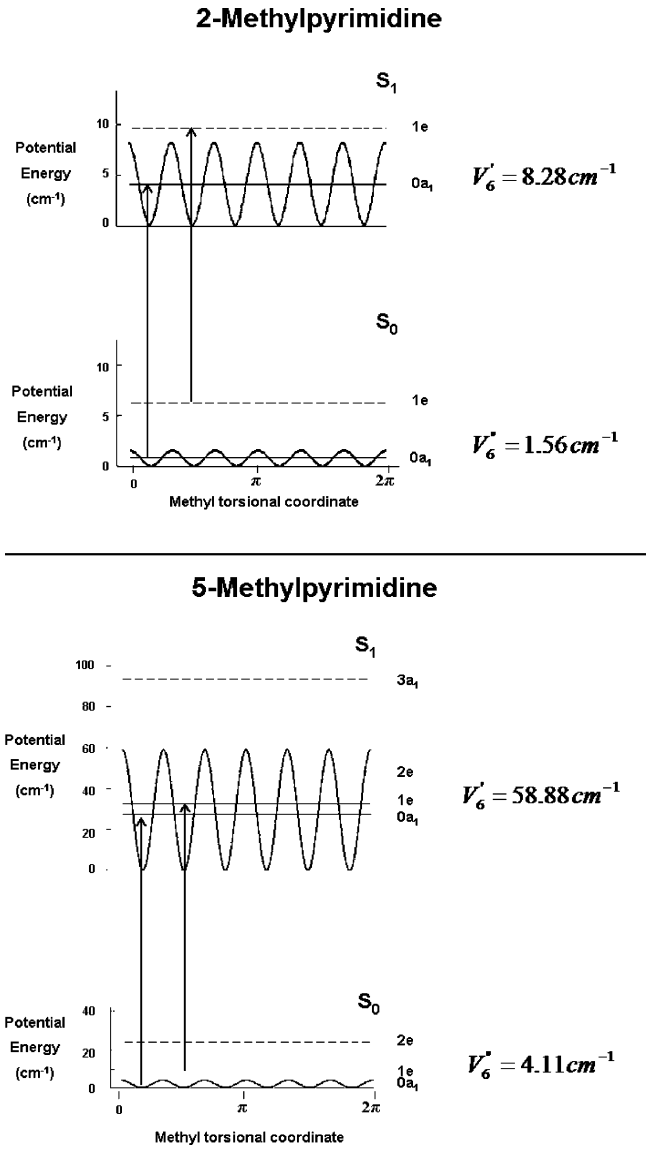

Figure 8. Torsional energy surfaces of 2MP and 5MP in both electronic states.

be resolved, identified, and approximately fit by an appropriate Hamiltonian. But since the spectra of 2MP and 5MP are significantly more perturbed than that of pyrimidine itself, we can safely conclude that methyl torsions enhance ISC in the isolated molecule and increase its rate. A similar finding has been made for the case of IVR by Parmenter and co-workers.[33] These authors argued that the increased IVR rate in molecules like *p*-fluorotoluene is primarily a reflection of a larger number of available states that can "couple through the exchange of energy between ring vibrations and internal rotation".[33]

Calculated densities of triplet vibrational states in the vicinity of the zero point vibrational level of the S_1 state are, according to the Haarhoff formula,[34] ∼0.60, ∼8.6, and ∼67 levels/cm^{-1} for pyrimidine, pyrazine, and 2MP respectively.

Unfortunately, groups of lines are so mixed and congested in the spectra of 2MP and 5MP that it is difficult to identify their JK_aK_c parentage and therefore to determine their zero-order character using the elegant Lawrance−Knight[35] deconvolution procedure. Application of this procedure to pyrimidine yielded zero-order energies spanning up to 1 GHz and spin−orbit couplings (SOC) matrix elements lying between 0 and 100 MHz.[9] However, it is still possible to extract some information

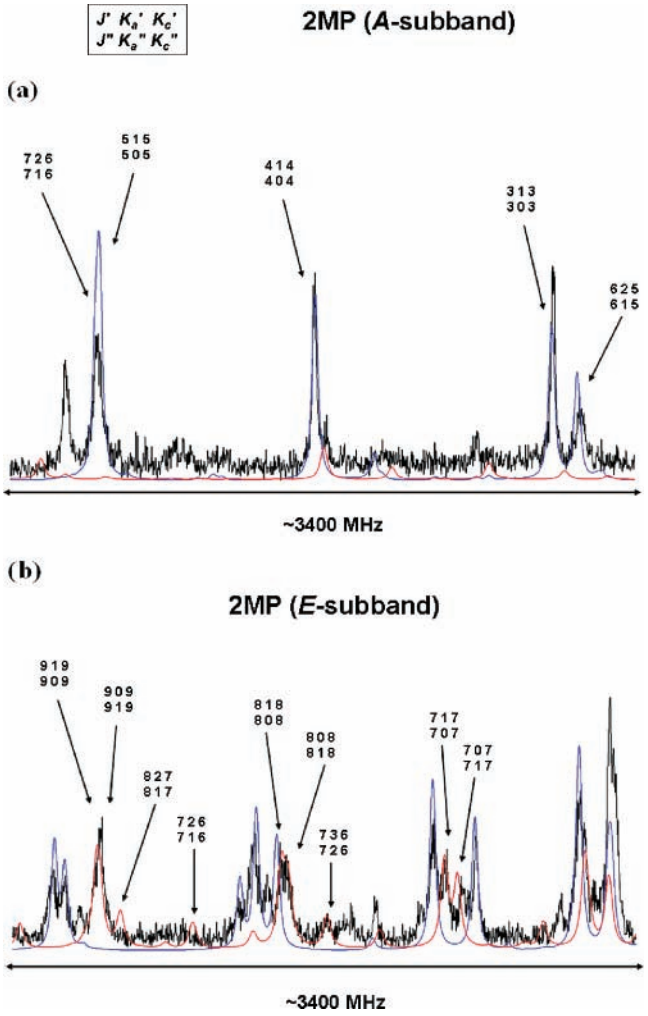

Figure 9. Intersystem crossing in the high-resolution electronic spectrum of 2-methylpyrimidine. The labeling of the transitions follows the quantum number pattern described in the box. (a) The *A* sub-band exhibits some extra lines next to the simulated transitions. (b) The *E* sub-band exhibits some frequency shifts and the degeneracy of the main transitions is broken.

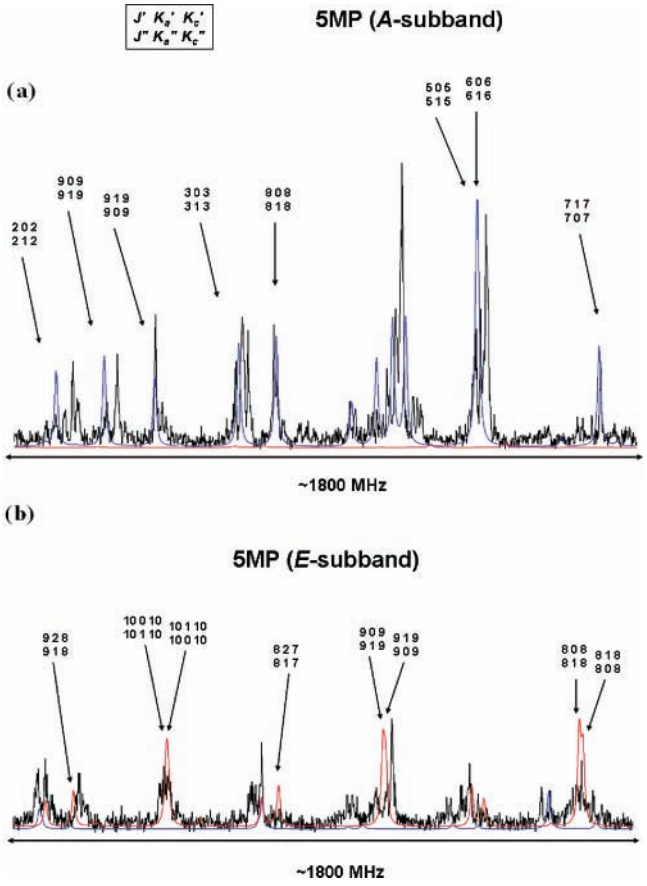

Figure 10. Intersystem crossing in the high-resolution electronic spectrum of 5-methylpyrimidine. The labeling of the transitions follows the quantum number pattern described in the box. (a) The *A* sub-band exhibits extra lines around the simulated transitions forming localized "clumps". (b) The *E* sub-band exhibits inhomogeneous broadening of peaks.

about the analogous process in the methylpyrimidines from the existing data. Figure 9 shows a comparison of selected regions of the *A* and *E* sub-bands in 2MP; Figure 10 shows a similar comparison for 5MP. Contrasting the two *A* sub-bands, we see that the spectra exhibit many "extra" lines as well as "main" lines; the individual standard deviations range from 1 to 100 MHz, equivalent to a lifetime of the order of 1 ns or so. At most, then, individual SOC matrix elements in the methylpyrimidines do not seem to be much larger than those in pyrimidine itself. On the other hand, we see that the number of perturbations is much larger than in pyrimidine, and that this number increases still further in the two *E* sub-bands, leading to an apparent inhomogeneous broadening of individual "zero-order" lines in the spectrum and the formation of "clumps".[36] Clump widths approaching 100 MHz are observed, apparently deriving from a higher density of states compared with the *A* sub-bands. Finally, we note that the number of perturbations is enhanced in 5MP, relative to 2MP, which may be a consequence of the significant difference in their torsional barriers in the S_1 state. A more quantitative assessment of the factors responsible for these dynamics will require microwave-optical double resonance experiments to disentangle the spectra.

5. Summary

2MP and 5MP reveal intersystem crossing dynamics upon electronic excitation because of extra lines and line broadenings observed in their fully resolved $S_1 \leftarrow S_0$ fluorescence excitation spectra. Both spectra were found to be more congested than that of pyrimidine because of the low-frequency motion of the attached methyl group. From the fits of the spectra, the V_6 methyl torsional barriers were determined for both molecules in their S_0 and S_1 electronic states. 5MP has a significantly larger barrier in its S_1 state than does 2MP, resulting in a higher density of coupled states and enhanced ISC in the isolated molecule.

Acknowledgment. Giacinto Scoles has been a tremendous champion (and practitioner) of high-resolution spectroscopy over the years, and we are grateful for his support. We also thank David R. Borst (INTEL) and David F. Plusquellic (NIST) for their helpful suggestions on the *lbrot* and JB95 fitting programs used for the data analysis, and the Koei Chemical Company for the kind donation of the 2-methylpyrimidine sample used in our experiments. Jim Pfanstiel and Jeff Tomer contributed to the early development of this project. This work has been supported by NSF (CHE-0615755).

References and Notes

(1) Innes, K. K.; Ross, I. G.; Moomaw, W. R. *J. Mol. Spectrosc.* **1988**, *132*, 492.

(2) Kommandeur, J.; Majewski, W. A.; Meerts, W. L.; Pratt, D. W. *Annu. Rev. Phys. Chem.* **1987**, *38*, 433, and references therein.

(3) Nesbitt, D. J.; Field, R. W. *J. Phys. Chem*. **1996**, *100*, 12735.
(4) Lahmani, F.; Tramer, A.; Tric, C. *J. Chem. Phys.* **1974**, *60*, 4431.
(5) Chaiken, J.; Benson, T.; Gurnick, M.; McDonald, J. D. *Chem. Phys. Lett.* **1979**, *61*, 195.
(6) ter Horst, G.; Pratt, D. W.; Kommandeur, J. *J. Chem. Phys.* **1981**, *74*, 3616.
(7) Matsumoto, Y.; Spangler, L. H.; Pratt, D. W. *Laser Chem.* **1983**, *2*, 91.
(8) Riedle, E.; Neusser, H. J.; Schlag, E. W. *J. Phys. Chem.* **1982**, *86*, 4847.
(9) Konings, J. A.; Majewski, W. A.; Matsumoto, Y.; Pratt, D. W.; Meerts, W. L. *J. Chem. Phys.* **1988**, *89*, 1813.
(10) van der Meer, B. J.; Jonkman, H. Th.; Kommandeur, J.; Meerts, W. L.; Majewski, W. A. *Chem. Phys. Lett.* **1982**, *92*, 565.
(11) de Souza, A. M.; Kaur, D.; Perry, D. S. *J. Chem. Phys*. **1988**, *88*, 4569.
(12) McIlroy, A.; Nesbitt, D. J. *J. Chem. Phys*. **1989**, *91*, 104.
(13) McIlroy, A.; Nesbitt, D. J.; Kerstel, E. R. Th.; Pate, B. H.; Lehmann, K. K.; Scoles, G. *J. Chem. Phys*. **1994**, *60*, 2596.
(14) Lehmann, K. K.; Scoles, G.; Pate, B. H. *Annu. Rev. Phys. Chem*. **1994**, *45*, 241.
(15) Green, W. H., Jr.; Moore, C. B.; Polik, W. F. *Annu. Rev. Phys. Chem*. **1992**, *43*, 591.
(16) Majewski, W. A.; Pfanstiel, J. F.; Plusquellic, D. F.; Pratt, D. W. In *Laser Techniques in Chemistry;* Rizzo, T. R., Myers, A. B., Eds.; J. Wiley & Sons: New York, 1995; p 101.
(17) Bandy, R. E.; Nash, J.; Zwier, T. S. *J. Chem. Phys*. **1991**, *95*, 2317.
(18) Bandy, R. E.; Garrett, A. W.; Lee, H. D.; Zwier, T. S. *J. Chem. Phys*. **1992**, *96*, 1667.
(19) Borst, D. R. Ph.D. Thesis. University of Pittsburgh, 2001.
(20) Plusquellic, D. F. *Jb95 spectral fitting program*; NIST: Gaithersburg, MD; http://physics.nist.gov/jb95.
(21) Spangler, L. H.; Pratt, D. W. In *Jet Spectroscopy and Molecular Dynamics*; Hollas, J. M., Phillips, D., Eds.; Chapman & Hall: London, 1995; pp 366−398.
(22) Gordy, W.; Cook, R. L. *Microwave Molecular Spectra*; John Wiley & Sons: New York, 1984; pp 607−617.
(23) Bunker, P. R.; Jensen, P. *Molecular Symmetry and Spectroscopy*, 2nd ed.; NRC Research Press: Ottawa, 1998; p 511.
(24) In an earlier report [Tan, X.-Q.; Pratt, D. W. *J. Chem. Phys*. **1994**, *100*, 7061], it has been shown that some molecules like the methylpyrimidines exhibit a precessional motion of the symmetry axis of the top with respect the C_2 symmetry axis of the frame, originating a precessing angle θ. We neglect this effect here.
(25) Caminati, W.; Cazzoli, G.; Troiano, D. *Chem. Phys. Lett*. **1976**, *43*, 65.
(26) Bitto, H.; Gfeller, S. *Chem. Phys. Lett.* **1997**, *265*, 600.
(27) Caminati, W.; Cazzoli, G.; Mirri, A. M. *Chem. Phys. Lett*. **31**, 104 (1975).
(28) Frisch, M. J.; Trucks, G. W.; Schlegel, H. B.; Scuseria, G. E.; Robb, M. A.; Cheeseman, J. R.; Montgomery, J. A., Jr.; Vreven, T.; Kudin, K. N.; Burant, J. C.; Millam, J. M.; Iyengar, S. S.; Tomasi, J.; Barone, V.; Mennucci, B.; Cossi, M.; Scalmani, G.; Rega, N.; Petersson, G. A.; Nakatsuji, H.; Hada, M.; Ehara, M.; Toyota, K.; Fukuda, R.; Hasegawa, J.; Ishida, M.; Nakajima, T.; Honda, Y.; Kitao, O.; Nakai, H.; Klene, M.; Li, X.; Knox, J. E.; Hratchian, H. P.; Cross, J. B.; Bakken, V.; Adamo, C.; Jaramillo, J.; Gomperts, R.; Stratmann, R. E.; Yazyev, O.; Austin, A. J.; Cammi, R.; Pomelli, C.; Ochterski, J. W.; Ayala, P. Y.; Morokuma, K.; Voth, G. A.; Salvador, P.; Dannenberg, J. J.; Zakrzewski, V. G.; Dapprich, S.; Daniels, A. D.; Strain, M. C.; Farkas, O.; Malick, D. K.; Rabuck, A. D.; Raghavachari, K.; Foresman, J. B.; Ortiz, J. V.; Cui, Q.; Baboul, A. G.; Clifford, S.; Cioslowski, J.; Stefanov, B. B.; Liu, G.; Liashenko, A.; Piskorz, P.; Komaromi, I.; Martin, R. L.; Fox, D. J.; Keith, T.; Al-Laham, M. A.; Peng, C. Y.; Nanayakkara, A.; Challacombe, M.; Gill, P. M. W.; Johnson, B.; Chen, W.; Wong, M. W.; Gonzalez, C.; Pople, J. A. *Gaussian 03*, revision B.05; Gaussian, Inc.: Wallingford, CT, 2003.
(29) Borst, D. R.; Pratt, D. W. *J. Chem. Phys*. **2000**, *113*, 3658.
(30) See, for example, Sinclair, W. E.; Pratt, D. W. *J. Chem. Phys*. **1996**, *105*, 7942 for the contrasting case of aniline.
(31) Alvarez-Valtierra, L.; Yi, J. T.; Pratt, D. W. *J. Phys. Chem.* **2006**, *110B*, 19914.
(32) For details of the *Atoms in Molecules* calculations, see, for example (a) Cioslowski, J.; Piskorz, P.; Rez, P. *J. Chem. Phys*. **1997**, *106*, 3607 and (b) Cioslowski, J.; Stefanov, B. B. *J. Chem. Phys*. **1996**, *105*, 8741.
(33) Moss, D. B.; Parmenter, C. S. *J. Chem. Phys*. **1993**, *98*, 6897 and references therein.
(34) Haarhoff, P. C. *Mol. Phys*. **1964**, *7*, 101.
(35) Lawrance, W. D.; Knight, E. W. *J. Phys. Chem*. **1985**, *89*, 917.
(36) This term has been extensively used for clusters of lines in spectral chaos and dynamics. See, for example, Sundberg, R. L.; Abramson, E.; Kinsey, J. L.; Field, R. W. *J. Chem. Phys*. **1985**, *83*, 466.